### Title

EcoIP: An open source image analysis toolkit to identify different stages of plant phenology for multiple species with pan-tilt-zoom cameras




### Journal

Ecological Informatics, 15(May 2013)

### ISSN

15749541



### Authors

Granados, Joel A.
Graham, Eric A.
Bonnet, Philippe
et al.



### Publication Date

2013-05-01

### DOI

10.1016/j.ecoinf.2013.03.002

Peer reviewed

Ecological Informatics 15 (2013) 58–65

Contents lists available at SciVerse ScienceDirect

Ecological Informatics

journal homepage: www.elsevier.com/locate/ecolinf

# EcoIP: An open source image analysis toolkit to identify different stages of plant phenology for multiple species with pan–tilt–zoom cameras

Joel A. Granados [a,*], Eric A. Graham [b], Philippe Bonnet [a], Eric M. Yuen [b], Michael Hamilton [c]

[a] IT University of Copenhagen, Rued Langgaards Vej 7, 2300 Copenhagen, Denmark.
[b] Center for Embedded Networked Sensing, University of California, Los Angeles, 3563 Boelter Hall, Los Angeles, CA 90095-1596, USA
[c] Blue Oak Ranch Reserve, University of California Berkeley, 23100 Alum Rock Falls Road, San Jose, CA 95127 USA

ARTICLE INFO

*Article history:*
Received 11 December 2012
Received in revised form 14 March 2013
Accepted 15 March 2013
Available online 24 March 2013

*Keywords:*
Phenology
Digital photography
Camera
Onset ending date
Color transformation
Bayesian analysis

ABSTRACT

Because of the increased number of cameras employed in environmental sensing and the tremendous image output they produce, we have created a flexible, open-source software solution called EcoIP to help automatically determine different phenophases for different species from digital image sequences. Onset and ending dates are calculated through an iterative process: (1) training images are chosen and areas of interest identified, (2) separation of foreground and background is accomplished based on a naive Bayesian method, (3) a signal is created based on the separation model and (4) it is then fit to a sigmoid that contains the dates of interest. Results using different phenological events of different species indicate that estimated dates fall within a few days of the observed dates for most cases. Our experiments indicate that color separability and scene illumination are contributing factors to this error. EcoIP is implemented as an open platform that encourages anyone to execute, copy, distribute, study, change, and/or improve the application.



## 1. Introduction

Plant phenology is one of the most responsive and easily observable traits in nature that are impacted by changing climate (Badeck et al., 2004). Indeed, plant phenology relates strongly to primary productivity and is sensitive to microclimatic variations, thus its study is vital to understanding species responses, ecosystem function, and the effects of climate (Wright et al., 1999). The interest in plant phenology and global climate change has increased significantly in recent years, especially with estimates of the advancing initiation of spring activity by both ground-based (Root et al., 2003; Walther et al., 2002) and satellite observations (Slayback et al., 2003; Stöckli and Vidale, 2004). The new U.S. National Phenology Network (USA-NPN, www.usanpn.org; Betancourt et al., 2007; Schwartz et al., 2012) is devoted to observing continental-scale trends in plant systems and growth dynamics.

Ideally, the best way to observe large-scale changes in phenological patterns with climate change is with remote sensing applications that are linked to ground-based measurements. Indeed, the manual collection of phenological data provides important information at the organism level while satellite imagery is captured over wide areas but at low spatial resolution, often too coarse to detect species and community level responses (Badeck et al., 2004). The use of new technology is being investigated to scale up (Allen et al., 2007) and standardize ground-based measurements by using a subset of species (USA-NPN, www.usanpn.org; Betancourt et al., 2007; Schwartz et al., 2012), and by modeling local climatic conditions (Jolly et al., 2005). Though methods are still lacking, the use of visible light digital cameras holds promise (Richardson et al., 2007).

Color in digital photography, computer vision and plant physiology have been used in studies that range from the extraction of individual concealed leaves in an image (Camargo et al., 2005) to assessing the forest under story (Liang et al., 2011). Simple image processing techniques are making standard the use of digital cameras for phenological event detection (Graham et al., 2009; Morisette et al., 2009; Richardson et al., 2007).

Agriculture is at the forefront of the use of image processing (Slaughter et al., 2008). Automation through digital photography was seen as early as 1995 in a weed detection application (Woebbecke et al., 1995). The automatic identification and control of unwanted species also occur in precision agriculture (Granitto et al., 2000; Swain et al., 2011) with concurrent work on the relation between leaf color and nutrient deficiencies (Wiwart et al., 2008) and automatic identification of the visual symptoms of plant disease (Camargo and Smith, 2008).

Many ad-hoc methods have been developed for using color to examine targeted aspects of plant health and phenology (e.g., Camargo and Smith, 2008; Ide and Oguma, 2010). Color is attractive because calculating values in an image is straightforward and many open-source software packages have functions that facilitate this analysis, such as the Python Imaging Library (Secret Labs AB; Linköping, Sweden; www.pythonware.com), and the R environment (R Development Core Team, 2012). However, using images captured in natural environments

* Corresponding author.
*E-mail address:* jogr@itu.dk (J.A. Granados).

1574-9541/$ – see front matter © 2013 Elsevier B.V. All rights reserved.
http://dx.doi.org/10.1016/j.ecoinf.2013.03.002

has some disadvantages such as color shifts caused by illumination changes which disrupt color-based analysis (Richardson et al., 2007), and displacements in regions of interest (ROI) caused by plant growth or movement by wind which requires repeated manual segmentation (Ide and Oguma, 2010). Solutions to these problems include the projection into other color indexes like $g_{cc}$ (Sonnentag et al., 2011) and transformations to other color spaces like CIE L*a*b* (Commission Internationale d'Eclairement, 1986), which have been used to increase stability when dealing with illumination issues (Sonnentag et al., 2011) and have been shown to greatly contribute toward an optimal segmentation process (Panneton and Brouillard, 2009). There are also many ways to automate image segmentation (Cheng et al., 2001; Litwin et al., 2001) that address plant displacement. However, no single color transformation or segmentation method may be able to capture all the phenological events of a single species (e.g., green-up, flowering, senescence), much less that of multiple species that may be captured within one or several images.

The recent expansion of imaging hardware, such as portable and Internet-connected visible light digital cameras, coupled with methods such as repeat photography and digital image processing, provide the means for detecting a wide range of scales of plant phenology, from mosses (Graham et al., 2006) to forests (Richardson et al., 2007). Indeed, visible-light digital cameras are becoming commonplace in research for quantitatively describing vegetation (Crimmins and Crimmins, 2008).

A few fixed digital cameras capturing plant images once or twice a day creates a data stream that can be readily hand-processed with excellent results (Graham et al., 2010). The proliferation of fixed-perspective Internet-connected cameras that are placed in either ecological areas or human-dominated systems is creating a situation where the data stream is approaching a limit after which it is no longer manually controllable. A new generation of inexpensive robotic pan–tilt–zoom (PTZ) cameras can now be employed to maintain high-resolution panoramic displays of natural environments (Song et al., 2006), creating a data stream that is orders of magnitude greater than a fixed view camera. For example, a downward-facing camera on a tower that can pan 350°, tilt 90°, and has a 10-× zoom, may have a 10° view angle and thus can collect many hundred unique-location images from a single vantage point. Thus, many more species and phenological events may be captured with a PTZ camera at the cost of much larger and potentially unwieldy image data sets being created.

Inspired by the need of investigators working in plant phenology in their efforts to use ground-based images for scaling up to regional phenomena coupled with the increased number of cameras used in environmental sensing and the tremendous image output of PTZ cameras, we have created a flexible, open-source software solution called EcoIP to use images to determine multiple phenophases for different species. It has been created specifically to address the lack of an open-source automated system for plant phenology and its objectives directly relate to ongoing research on segmentation and color transformations in this field. The paper is organized in the following way: Section 2 provides details on the process we followed and how we used the Naive Bayesian Model in EcoIP. In Section 3 we describe our results and in Section 4 we outline their relevance within the current state of the art. There is a short description of the future work in Section 5 and we finish with conclusions.

## 2. Materials and methods

### 2.1. Processing images with EcoIP

The input for the Ecological Image Processing (EcoIP) software toolkit (Granados, 2012b) is a series of images taken of the same location, with the same camera and at the same time of day. Through an iterative process (Fig. 1) EcoIP creates a representation of the image series which is then used to estimate onset and ending dates of phenophases.

#### 2.1.1. Image training set generation

The creation of Image Training Sets (ITS) is the first step in the iterative process to find an optimal model that describes a phenophase. We generate it by selecting a subset of images that contain different types of scenarios of one year in an image series (winter, summer, sunny, cloudy, rainy, foggy…). We then manually identify a subgroup of pixels from individual images within the ITS as representative of a phenophase with the aid of an annotation tool (Granados, 2012a; Annotation tool for Matlab) that allows for the selection of pixels by enclosing them with annotated polygons or annotations. Pixels that represent the phenophase of interest are labeled as foreground (FG; e.g., leaves and flowers) and pixels that represent everything else are labeled as background (BG; e.g., sky, soil, and surrounding plants). Care is taken when creating the training set to include enough images to capture a representative sample of the changing

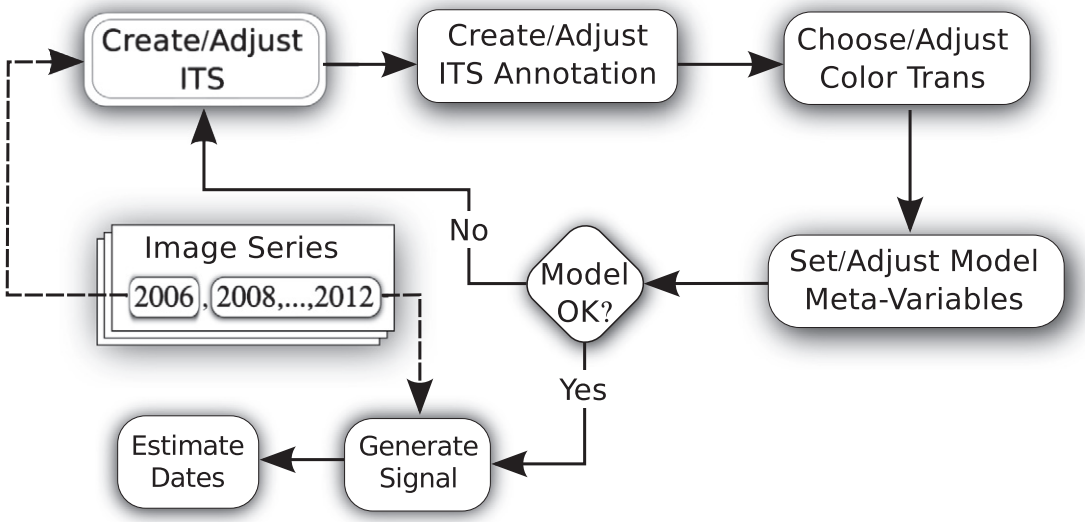


**Fig. 1.** EcoIP data processing work-flow begins with creating the ITS. Models and signals are created with input from image series. Model creation is iterative. Data used for model creation is ignored in signal generation.

phenology (e.g., beginning, middle, and end of the phenophase of interest) and though filtering noisy (foggy and rainy) images is common, we include them in the training set.

#### 2.1.2. Choosing the color transformation

We determine frequency distributions of BG and FG pixels for each color transformation (calculated from original RGB coordinates) supported by EcoIP. These are used to manually select the appropriate transformation (Table 1) which is rated based on its ability to maximally separate BG and FG pixels for each phenology and species of interest (Fig. 2). After choosing a color transformation we adjust model variables such as Bayesian class prior probabilities, smooth filter characteristics, number of bins for frequency analysis and model accuracy calculation characteristics. These adjustments directly affect the accuracy of the resulting model.

#### 2.1.3. Naive Bayesian model generation

The creation of a Naive Bayesian Model (NBM) is done automatically by EcoIP and results in an R (R version 2.15.0, R Team, 2012) data file. By default an S-fold cross-validation (Bishop, 2007, page 33) is used to calculate the false positives (incorrectly classified FG pixels) and the false negatives (incorrect BG pixels) of the training data and is used to rate and compare models. Their values are indicated relative to the total number of pixels examined and can be used to predict how the model will behave with new data for the same phenophase. Re-annotating or modifying the images in the ITS, selecting a different color transformation, and further adjustments to EcoIP variables are part of the iterative process (Fig. 1) to determine an optimal NBM that is chosen among the results of the manual iterations and that minimizes the false positives and false negatives for specific phenophase.

#### 2.1.4. Phenology signal generation

Each NBM is then applied to a series of new images to classify each pixel as either FG or BG resulting in a new series of binary (black and white) images. Counts of binary pixels are used to create proportion values for each image by dividing the number of identified FG pixels by the total image pixels. "Blob" count values, which require a morphological transformation (Jähne and Haußecker, 2000, page 483) of the original binary image, are also created by counting the number of contiguous areas of white (FG) pixels in the resulting binary image. The signal is then a sequence of these values related to an image and a date. It is important to note that data used to create the models are set aside (Fig. 1) when calculating the values (Bishop, 2007, page 32) to avoid a preexisting bias towards the data used for model creation.

Our data contained species captured by several signals. In these cases it was of interest to consider the phenological behavior of a set of signals effectively increasing the scale given by just one image frame. We created a consolidated signal by averaging the values of a date of individual signals. The resulting signal, like the individual signals, is a sequence of values.

**Table 1**
Summary for model values. Sample size is the range of years used for each phenophase. We display the color transformation that resulted in the best model for each phenophase. The average error (in days) is the average absolute value of the difference between estimated dates and observed dates for each phenophase.

| Phenophase | Sample size | Color transform | Average error |
|---|---|---|---|
| Summer 'oak canopy' | 2009–2010 | CIE L*a*b* | 2.00 |
| Autumn 'oak canopy' | 2009–2010 | CIE L*a*b* | 1.25 |
| Summer 'oak close-up' | 2007–2010 | Excess green | 1.39 |
| Autumn 'oak close-up' | 2007–2011 | CIE L*u*v* | 3.64 |
| Bracken fern | 2008–2011 | Excess green | 2.79 |
| Wallflower | 2007–2011 | YCbCr | 2.84 |
| Average total error | | | 2.78 |

#### 2.1.5. Estimating phenology dates

Phenological dates are estimated by a semiautomatic process of fitting the data with a sigmoid function (Eq. (1)) and then identifying the inflection points in these functions (Ide and Oguma, 2010; Richardson et al., 2007). The first inflection point in the phenological signal (onset date) is located where the second derivative changes sign in the first sigmoid (positive Eq. (1)) and the second point (end date) is where the second derivative changes sign in the second sigmoid (negative Eq. (1)). This places the inflection point midway between the maximum and minimum of the sigmoid. The 'a' and 'b' values in Eq. (1) define the vertical range, 'c' controls horizontal translation of inflection points, 'd' controls steepness and 'x' is time.

$$f(x) = a \pm \frac{b}{1 + e^{(c - d*x)}} \tag{1}$$

For the consolidated signals we implemented two approaches for estimating the phenological dates: the first is the process that was just described applied to a consolidated signal. The second estimates the onset date and ending date of a phenophase with the minimum onset date and maximum ending date of the component signals.

### 2.2. Applying EcoIP

#### 2.2.1. Gathering images

We used two PTZ networked video cameras (Model VB-C50iR, Canon U.S.A., Lake Success, New York) placed on 30 m fiberglass towers in the University of California James Reserve located in the San Jacinto Mountains of southern California (33° 48′ 30″ N, 116° 46′ 40″ W) at 1658 m elevation in a mixed conifer and hardwood forest. The cameras were installed at different times starting in 2005. The reserve acts as a testbed for technology developed by the Center for Embedded Networked Sensing (CENS), an NSF funded Science and Technology Center located at the University of California, Los Angeles (http://research.cens.ucla.edu).

Acquired images were sent to a repository at CENS where each one contained meta-data describing the time of day, the PTZ coordinate, and the location of the camera inside the reserve. The files which had a resolution of 480 × 640 pixels were kept in Joint Photographic Experts Group (JPEG; ITU, 1992) format with a minimum amount of compression. In general we collected images ranging from 2006 to 2012. From the repository we created multiple series of images (PTZ-series) for pan–tilt–zoom coordinates which make up our raw input and contain species of interest. As in other digital repeat photography projects (Ide and Oguma, 2010 and Sonnentag et al., 2011) there were missing data due to adverse weather conditions, failures in hardware and software, and changing on-site data collection policies. Table 1 summarizes the ranges of each PTZ-series for each selected species and phenology.

#### 2.2.2. Selected species and phenologies

To demonstrate the flexibility of analysis we selected three species that presented noticeable (in the visual spectrum) phenological changes, had a minimum of photography issues and continued for more than one year: oak (*Quercus* sp.), bracken ferns (*Pteridium aquilinum*), and wallflowers (*Erysimum capitatum*) (Fig. 3). The perennial oak and bracken fern were different because we could predict where the leaves would emerge for the oak whereas for the underground rhizome of the bracken fern, such predictions were difficult and so a more "zoomed out" approach was necessary. For the annual wallflower, the uncertainty of location was taken to an even greater extreme requiring a larger canvassing of the area with images.

Phenophases for the three species included the green-up and senescence for the oak, the green-up and senescence for the bracken ferns, and the blooming period for the wallflowers (mid-summer). We collected two types of PTZ-series for the oak: a full canopy view ('oak canopy') and a close-up of the canopy ('oak close-up') where

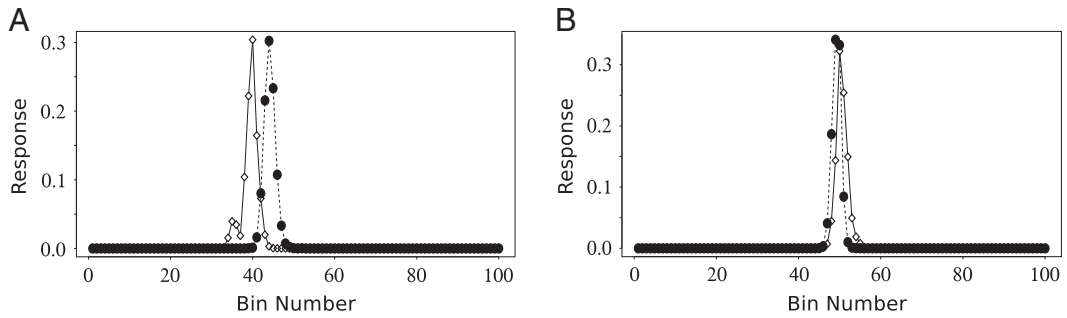


**Fig. 2.** Examples of EcoIP's histogram comparison between background (open symbol) and foreground (closed circle) of two color transformations. The color transformation values are binned to 100 values and the response represents the proportion of pixels per bin, normalized by the total number of pixels in the image. (A) Displays the second (*a) channel in the CIE L*a*b* color space and is an example of good separability between FG and BG. (B) Displays the excess green color index and is an example of a bad separability.

individual leaves could be isolated; we estimated summer and autumn colors in each.

The 'oak canopy' images (Fig. 3A) had an oak tree in the foreground and a view of the surroundings that included pines, other oaks, some bushes, remote mountains, and the sky in the background. The 'oak close-up' images (Fig. 3B) were zoomed such that oak leaves filled all of the image in summer while fallen leaves, debris, and snow were visible through the leafless canopy in winter. For both the 'oak canopy' and 'oak close-up' we trained a summer and autumn model, where the summer one used green leaves for their input and the autumn one used red ('oak canopy') and yellow ('oak close-up') leaves for theirs. We used different autumn colors for 'oak canopy' and 'oak close-up' because of different microclimates experienced between the two types of photographed individuals. This is further exacerbated by the camera's automatic adjustments controlled by drastically different lighting environments where everything in the 'oak canopy' image is modified by the excessive brightness of the sky as opposed to a more homogeneous frame for the 'oak close-up'.

The bracken ferns (Fig. 3C) were located in a meadow where they shared space with the wallflowers (Fig. 3D). Leaf litter from nearby trees (fallen branches, pine needles, and autumn leaves) constituted the background. We identified the green color of the ferns and the yellow of the wallflowers as the specific colors related to the growth phenology of the ferns and the flowering time for the wallflowers. For the wallflowers signals were generated from the resulting blob counts whereas for the rest of the species the initial proportions were used.

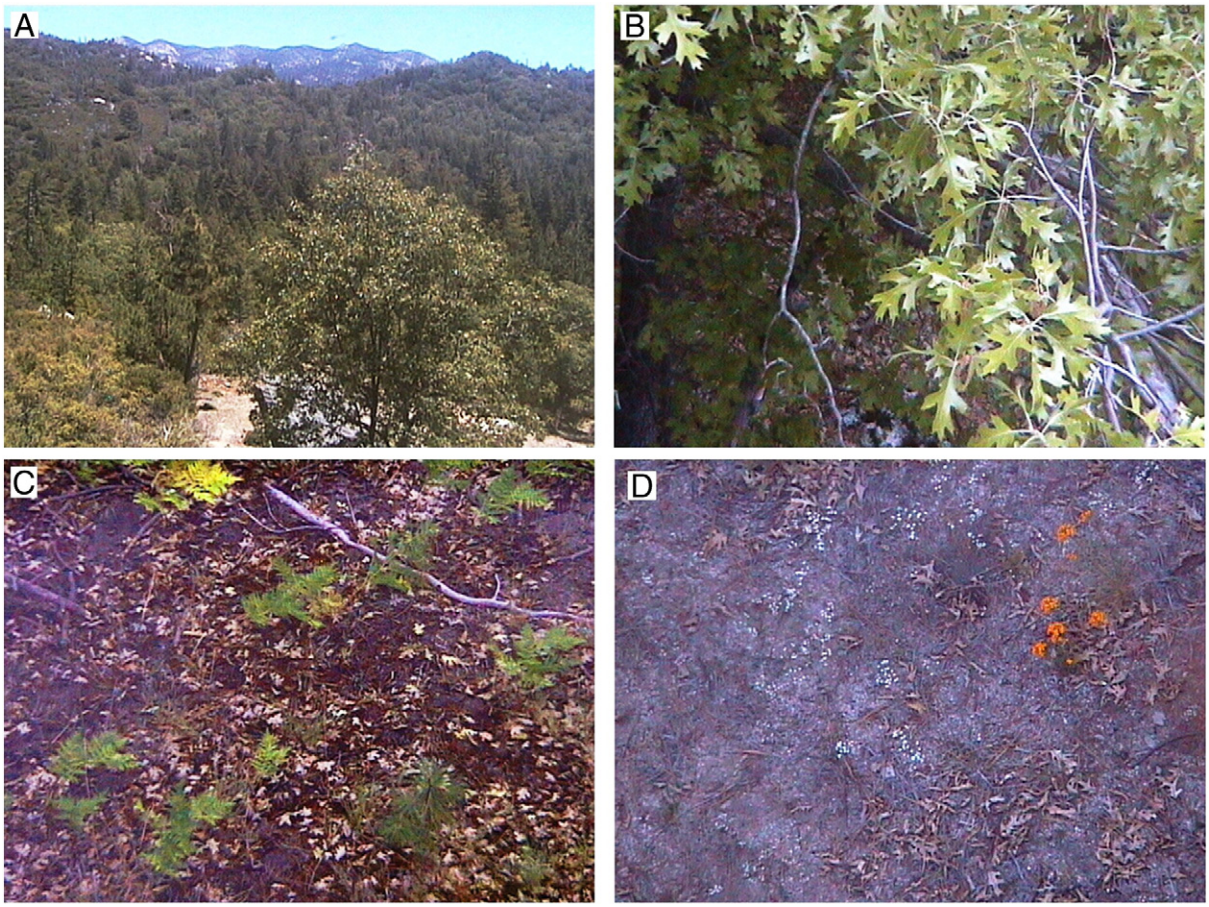


**Fig. 3.** Representative images captured from 3 PTZ cameras at the James Reserve. (A) Canopy of deciduous oak (*Quercus* sp.). (B) Close-up of deciduous oak (*Quercus* sp.). (C) Bracken ferns (*P. aqualinum*). (D) Yellow meadow wallflowers (*E. capitatum*).

From 2006 to 2012 over 700,000 images were collected of which 79,000 contained images of chosen phenologies. We further sifted the set into 1 series of 'oak canopy', 4 series of 'oak close-up', 8 series of ferns and 10 series of wallflowers. The 'oak canopy' was trained with a subset of the series while the 'oak close-up', fern and wallflower were trained with 1, 1 and 4 of their respective series. Given the proximity of the locations of the images of the fern and the wallflowers, we created consolidated PTZ-series for each.

### 2.3. Estimated vs. observed data

To generate our observed dates for the wallflowers we marked an onset date when we identified the first visible flower and an ending date when the last flower disappeared. For the ferns we marked an onset date when we saw the first green fern frond emerge from the soil and an ending date when we visually assessed that 90% of the green fronds had turned dark yellow or light brown.

For the summer 'oak canopy' we marked an onset date at the first signs of new leaves and an ending date when 90% of the canopy had lost its green and turned red. For the autumn 'oak canopy' we marked an onset date when 90% of the canopy had changed to red and an ending date when most of the leaves of the canopy had fallen. For the summer 'oak close-up' we marked an onset date when most of the emerging leaves turned green and an ending date when 90% of the leaves had turned yellow. For the autumn 'oak close-up' we marked an onset date when 90% of the leaves had lost their dark green color and turned either light green or yellow and an ending date when 90% of the leaves had fallen from the tree.

After determining the observed dates we calculated model accuracy by comparing them with the estimated dates calculated by the algorithm. For the consolidated case (ferns and wallflowers) we first calculated observed consolidated dates by considering an onset date as the minimum of all observed onset dates (per phenophase) and, in a similar way, considering an ending date as the maximum of all observed ending dates (per phenophase). We then compared the observed dates with the two approaches (Section 2.1.5) used to calculate the estimated dates.

## 3. Results

### 3.1. Size of ITS

To train the 'oak canopy' models we used the totality of one of the two years (Table 1) in the image series (294 images). Since images did not change on a daily basis we reduced this number to 124 (roughly 10 images per month) for 'oak close-up' in the hope of producing models with similar error values. By creating a model with a smaller error (summer 'oak close-up') than the one created with the larger ITS (summer 'oak canopy'), we show that we can get workable models with reduced image sets (Table 1).

### 3.2. Selected color transformations

We selected the color transformation based on the model error values (Table 2) and on EcoIP's histogram comparison (Fig. 2). As in other projects (Ide and Oguma, 2010; Panneton and Brouillard, 2009; Richardson et al., 2007) the excess green color index and the CIE 1976 L*a*b* (Commission Internationale d'Eclairement, 1986) color space optimized vegetation color analysis. These two color transforms were selected for all the green phenophases in our study (Table 1). Only in autumn 'oak close-up' and wallflower did we use different color transformations (Table 1).

### 3.3. Model error

The cross validation error (Table 2), used to compare models, provides hints at the behavior of the model with real data. We used the false negatives and false positives as accuracy measures based on the assumption that the distribution of the training and "real" data are the same, since the camera, the time of day and the location were the same for training and "real" data. Although the wallflower model appeared to have a poor cross validation error (Table 2), applying the blob count method suppressed the greater-than and smaller-than blobs to contribute to a well behaved average error of 2.84 (Table 1). The remainder of our experiments fell within 90% accuracy (Table 2) except for the autumn 'oak close-up' (25.32% false negatives) and autumn 'oak canopy' (17.61% false negatives) of which the autumn 'oak canopy', despite the 17.61%, led to a good average error of 1.25 (Table 1).

**Table 2**
Cross validation error. Percentage of false negatives (pixels that were misclassified as BG) and false positives (pixels that were misclassified as FG) calculated for each species phenophase.

| Phenophase | False negatives[a] | False positives[a] |
|---|---|---|
| Summer 'oak canopy' | 8.91 | 4.51 |
| Autumn 'oak canopy' | 25.32 | 0.31 |
| Summer 'oak close-up' | 2.11 | 1.38 |
| Autumn 'oak close-up' | 17.61 | 0.025 |
| Bracken fern | 5.13 | 1.20 |
| Wallflower[b] | 63.86 | 5.50 |

[a] Calculated using s-fold method (Bishop, 2007, page 33).
[b] Before blob analysis calculations.

### 3.4. Dates of phenophases

The average error for the combined experiments was 2.78 (Table 1), indicating that, on average, the estimated onset and ending dates fell within a range of ±2.78 d of the observed dates. The best results occurred for the autumn 'oak canopy' that had an error of 1.25 d and the worst value was for the autumn 'oak close-up' with 3.64 error value. This relatively poor performance is a result of an error of 24 days in the 2010 end of autumn date (Fig. 4) due to a noisy peak that is near and similar in size to the main signal. In Fig. 5 we compare the error distribution of all the studied phenophases.

### 3.5. Consolidated PTZ-series

The comparison of the consolidated observed dates with the ones estimated by the first approach (Section 2.1.5) resulted in an average error of 3.87 days and 3.5 days for the wallflowers and ferns respectively (Table 3). When we compared the consolidated observed dates with the ones estimated by the second approach (Section 2.1.5), we saw an average error of 2.9 days and 2.75 days for the wallflowers and ferns respectively (Table 3). These values coincide with the ones in Table 1 and represent the accuracy of our method for multiple PTZ-series of the same species.

## 4. Discussion

### 4.1. Phenology and the EcoIP toolkit

With the advent of new technology it is becoming easier to generate great amounts of digital image data. Pan–tilt–zoom cameras increasing resolution coupled with portable field data collection devices and large databases are creating situations where the amount of digital image data collected can exceed the capacity for prompt analysis. The method described in this paper, together with the EcoIP toolkit, contribute to the automation of phenological data analysis based on digital images by completely controlling the signal creation. The use of a Naive Bayesian Model to generate a probabilistic representation of a color transformation to determine the dates for phenophases allows rapid and robust model creation that directly translate into semi-automatic date estimations.

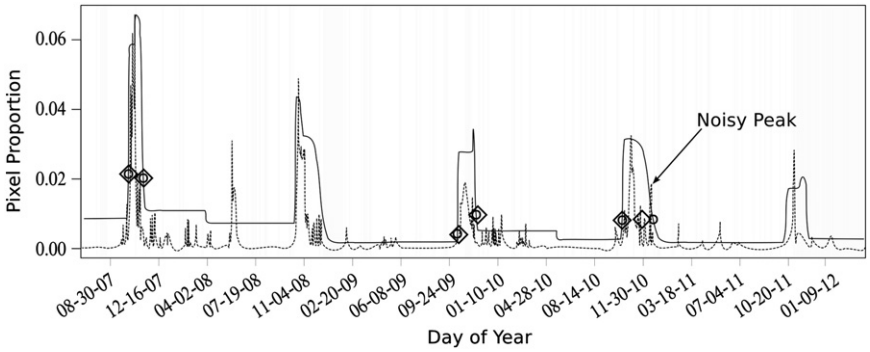


**Fig. 4.** Sigmoid fit (solid line) to the phenological signal (dotted line) of an autumn 'oak close-up'. Shaded areas represent missing data. Training was done with images from 2009. Circles are estimated dates and diamonds are observed dates for both the onset and ending of autumn in the 'oak close-up' image series. 2008 and 2011 not included due to missing data. Fit is particularly noisy in 2010 where there is a large difference between the estimated and observed ending date.

EcoIP is implemented as an open platform that encourages anyone to execute, copy, distribute, study, change, and/or improve the application (Granados, 2012b). The code is made available for download and examples are provided for every function to aid the user. EcoIP is designed as an R (R version 2.15.0, R Team, 2012) package and it can easily be installed in any platform where R is available. Help within EcoIP is provided with sample data and executable examples. Two data sets are included: One of an Oak and another of wallflowers.

EcoIP has a lot of room for improvement. One of its major weaknesses is that it focuses exclusively on color. It ignores other, potentially useful, aspects of the image like the temporal information (contained in the image series) that could be used to make decisions based on preceding and posterior images. The texture and shape of the FG and BG could be added as an additional dimension to the NBM. EcoIP is also constrained by the statistical model it uses. For the moment it only works with a naive Bayesian approach but there could be an increase in accuracy if we could experiment with approaches like support vector machines, FFT analysis, wavelet transform or neural networks.

### 4.2. Color transformations

In our experiments, there was no optimal color transformation that allowed separation of phenological events among species or even within species. For example, for the summer 'oak canopy' we used a version of the excess green color index (Richardson et al., 2007; Woebbecke et al., 1995) to detect green leaves, but in autumn we used CIE 1976 L*a*b* (Commission Internationale d'Eclairement, 1986) to detect the color change from green to red leaves. Indeed, color transformations influence image segmentation and posterior classification, and should be incorporated as yet another variable when doing these analysis as opposed to fixing it on one value.

EcoIP has not only tackled image series that are characteristically green (summer 'oak canopy', summer 'oak close-up' and ferns), it has also extended previous ecological work (Ide and Oguma, 2010; Richardson et al., 2007; Sonnentag et al., 2011) by estimating onset and ending dates of non-green phenophases (autumn 'oak canopy', autumn 'oak close-up' and wallflowers). Our results show that there are other color transformations (YCbCr, CIE L*u*v*) that are better equipped for segmenting these non-green phenophases and therefore a broader set of transformations should be considered when doing analysis of phenophases like the blooming period of flowers (wallflowers) and the autumn period in oaks (autumn 'oak close-up' or autumn 'oak canopy').

The choice of color transformation to analyze the phenophases of the 'oak canopy' and 'oak close-up' were different in order to maximize the signal and detect the timing of events with the greatest resolution. However, the ability to compare the two data streams analyzed with different methods may thus be compromised. The flexibility of EcoIP allows analysis with any choice of color transformation and so it is left up to the investigators using EcoIP to use the system as a tool for data exploration.

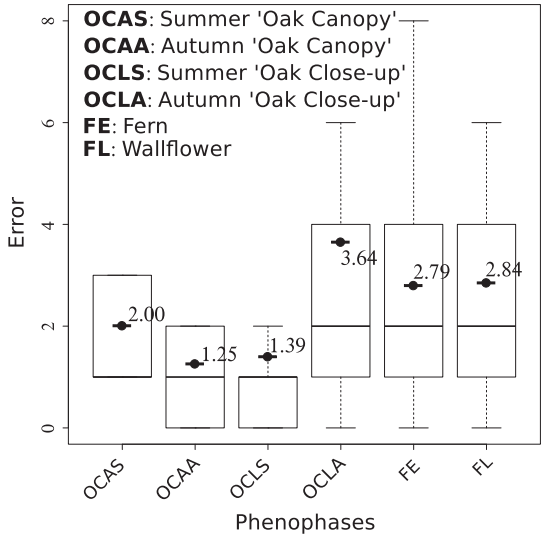


**Fig. 5.** Distribution of error values (in days) for each phenophase. Mean value is marked and displayed for each phenophase. Though outliers are not included in the figure, we include them in the mean value calculation.

### 4.3. Noise

While the color signals contain the underlying structure of the phenophases, they also contain noise (Fig. 6) which represent a high concentration of false positives and negatives. Noise in images is produced by natural changes in illumination, undesired automatic camera adjustments, and hardware failure. The choice of a color transformation that minimizes the effect of illumination (e.g., L*a*b, where luminance is separate from the color channels) can reduce naturally-occurring noise while color transformations with less separation of FG and BG (Fig. 2) resulted in a nearly random signal (data not shown). Mitigation of camera-created noise requires full control of the camera settings

**Table 3**
Average of the absolute value of the difference between the consolidated estimated dates and the observed dates. The consolidated sigmoid error is estimated from the consolidated signal inflection points (first approach, Section 2.1.5). The individual sigmoid error is estimated from minimum and maximum estimates (second approach, Section 2.1.5).

| Type | Consolidated sigmoid error | Individual sigmoid error |
|---|---|---|
| Fern consolidate | 3.50 | 2.75 |
| Wallflower consolidate | 3.87 | 2.90 |

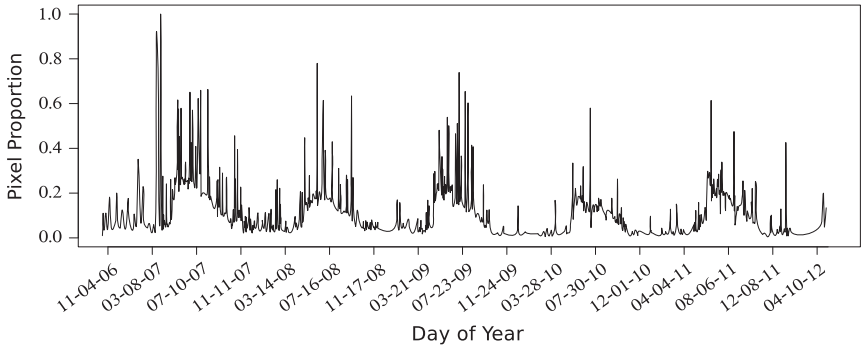


**Fig. 6.** Bracken fern raw signal. 2008 is ignored due to noisy values.

(aperture, exposure time, and white balance), which may not be possible in many situations where cameras are controlled by third parties (e.g., land owners or reserve managers). We also experienced hardware and software malfunctions: In Fig. 6, before the beginning of the 2007 season, there are uncommonly large signal responses caused by erroneous exposure times, erroneous aperture values or bad focus resulting in completely black or blurry images. Given the amount of ignored data due to lack of camera resilience and camera control, we argue that more emphasis should be placed on these two aspects to mitigate these types of errors.

An additional problem with images in natural areas is the impossibility to separate regions of interest based on color alone. For example, Fig. 7 has two peaks per season, which is caused by direct sunlight striking fallen leaves in the meadow that reflect a color that is nearly identical to the yellow of the wallflower. We reduced this effect by manually identifying and ignoring the erroneous signals. Something similar occurred with the colors in summer 'oak close-up' where autumn yellow and summer green were being classified as FG pushing the estimated ending summer date approximately one month after the observed one. Fig. 8 is used to compare the position of each element in the excess green color index. We see a large separation between greens of summer and the browns of bark and fallen leaves. But unfortunately, autumn yellow and summer green are in close proximity, which led to the misclassification. We see the same behavior in the summer 'oak canopy' where the green of the oak is classified as FG together with the greens of the distant pines. This however did not incur in any date miscalculation because the pine colors were constant throughout the summer.

### 4.4. Consolidating signals

The process of adding different local elements into a global response is a way to visualize the behavior of individuals with respect to their containing ecosystem. Our consolidated signal was aimed at giving global onset and ending dates for ferns and wallflowers. Results showed that the way the consolidation was done had an effect on the accuracy. While we expected the first approach (Section 2.1.5) to suppress erroneous responses (given the added data), we found that it increased the final error (Table 3). The averaging of noisy signals, together with the recalculation of inflection points resulted in a final error that surpassed the consolidation done with the second approach (Section 2.1.5). We therefore preferred it to determine the onset and ending dates of ferns and wallflowers. We see that we need to consider additional noise and error factors of procedures used to consolidate local measurements.

## 5. Future work

An increase in the accuracy of phenological date estimates can occur on several fronts. Computer vision features such as texture (Jähne, 2005, page 435), shape (Jähne, 2005, page 515), and even motion (Jähne, 2005, page 397) can mitigate or even completely remove some sources of noise in image series used for phenology. Motion and an understanding of the temporal characteristics of the phenomenon of interest are of particular interest given the characteristics of time series data. Motion features can separate ROIs (a moving branch compared to an immobile soil surface) and short-term situations, like the sun reflecting off a patch of fallen leaves, can be removed by incorporating temporal filtering (a flower persists in one location through many images whereas a sun fleck may move within a day or within a season).

One exciting possibility, after the automatic detection of colors within an image has been established with EcoIP, is to create a more independent ROI detector. In this way, images from PTZ cameras may be captured at a high frequency and in locations not pre-programed and then subsequently analyzed for ROIs. If nothing is found, then the image is discarded, reducing the transmission load from remote ecological reserves and reducing image storage needs. If an ROI is detected, then the image may be sent to a human operator for evaluation and feedback refinement of the NBM.

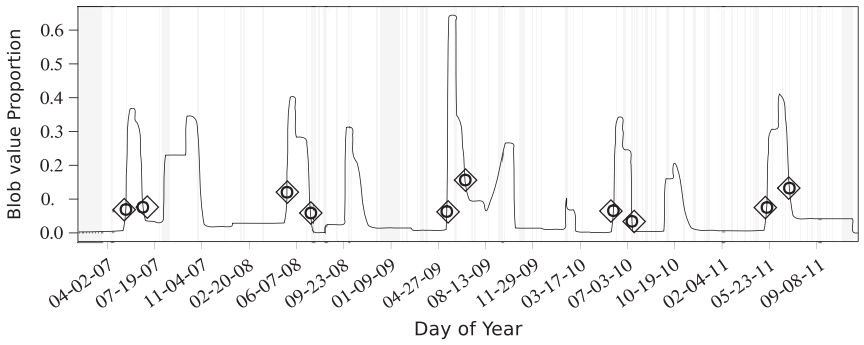


**Fig. 7.** Consolidated sigmoid fit of the wallflower signal from six independent PTZ image series. Circles on sigmoid are estimated dates and diamonds are observed dates for both the beginning and ending of the blooming period of the wallflower image series. Here we show a specific type of noise where there are two peaks per season instead of one.

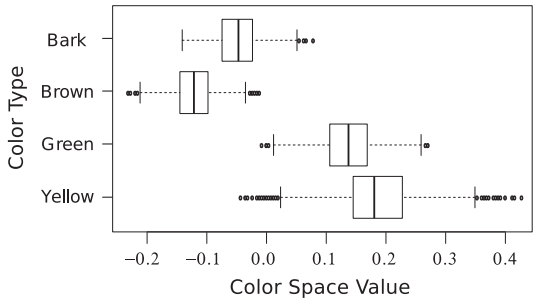


**Fig. 8.** Distribution of color values in the excess green color index for summer 'oak close-up'.

## 6. Conclusions

We have introduced EcoIP, a toolkit that calculates onset and ending dates of phenologies of interest based on pan–tilt–zoom image series. In our experiments the toolkit estimated with an overall error of 2.78 days from the observed date and was able to analyze phenophases with characteristic colors different than green. We consolidated individual image series to describe ecosystems that could not be captured in one scene. We found that color separability and scene illumination are contributing factors to the overall error. And we were able to effectively use initial false negative and false positive values to pinpoint usable models.

## Acknowledgments

The research leading to these results has received funding from INTERACT (grant agreement No 262693), under the European Union's Seventh Framework Program. A portion of this research was also supported by National Science Foundation award 0120778 to the Center for Embedded Networked Sensing at the University of California, Los Angeles.

## References

Allen, M.F., Vargas, R., Graham, E.A., Swenson, W., Hamilton, M., Taggart, M., Harmon, T.C., Rundel, P., Fulkerson, B., Estrin, D., 2007. Soil sensor technology: life within a pixel. Bioscience 57, 859–867.

Badeck, F.W., Bondeau, A., Bottcher, K., Doktor, D., Lucht, W., Schaber, J., Sitch, S., 2004. Responses of spring phenology to climate change. New Phytologist 162, 295–309.

Betancourt, J.L., Schwartz, M.D., Breshears, D.D., Brewer, C.A., Frazer, G., Gross, J.E., Mazer, S.J., Reed, B.C., Wilson, B.E., 2007. Evolving plans for the USA National Phenology Network. EOS. Transactions of the American Geophysical Union 88, 211.

Bishop, C.M., 2007. Pattern Recognition and Machine Learning, 6th edition.

Camargo, A., Smith, J.S., 2008. An image-processing based algorithm to automatically identify plant disease visual symptoms. Biosystems Engineering 102, 9–21.

Camargo, J., Meyer, G.E., Jones, D.D., 2005. Individual leaf extractions from young canopy images using Gustafson–Dessel clustering and genetic algorithm. Computers and Electronics in Agriculture 51, 66–85.

Cheng, H.D., Jiang, X.H., Sun, Y., Wang, J., 2001. Color image segmentation: advances and prospects. Pattern Recognition 34, 2259–2281.

CIE (Commission Internationale de l'Eclairage), 1986. Colorimetry, CIE Publication 15.22nd ed. Central Bureau of the Commission Internationale de l'Eclairage, Vienna (83 pp.).

Crimmins, M.A., Crimmins, T.M., 2008. Monitoring plant phenology using digital repeat photography. Environmental Management 41, 949–958.

Graham, E.A., Hamilton, M.P., Mishler, B.D., Rundel, P.W., Hansen, M.H., 2006. Use of a networked digital camera to estimate net $CO_2$ uptake of a desiccation tolerant moss. International Journal of Plant Sciences 167, 751–758.

Graham, E.A., Yuen, E.M., Robertson, G.F., Kaiser, W.J., Hamilton, M.P., Rundel, P.W., 2009. Budburst and leaf area expansion measured with a ground-based, mobile camera system and simple color thresholding. Environmental and Experimental Botany 65, 238–244.

Graham, E.A., Riordan, E.C., Yuen, E.M., Estrin, D., Rundel, P.W., 2010. Public internet-connected cameras used as a cross-continental ground-based plant phenology monitoring system. Global Change Biology 16, 3014–3023.

Granados, J.A., 2012a. An Annotation Tool for Matlab. (Copenhagen, http://github.com/Joelgranados/annotation, 27-Mar-2013).

Granados, J.A., 2012b. Ecological Image Processing (EcoIP). https://github.com/Joelgranados/EcoIP (27-Mar-2013).

Granitto, P.M., Navone, H.D., Verdes, P.F., Ceccatto, H.A., 2000. Weed Seeds Identification by Machine Vision. Universidad Nacional de Rosario.

Ide, R., Oguma, H., 2010. Use of digital cameras for phenological observations. Ecological Informatics 5, 339–347.

ITU, 1992. Information technology – digital compression and coding of continuous-tone still images – requirements and guidelines. Recommendation T.81.International Telecommunication Union, Genève, Switzerland (186 pp.).

Jähne, B., 2005. Digital Image Processing, 6th edition. .

Jähne, B., Haußecker, H., 2000. Computer Vision and Applications. A Guide for Students and Practitioners.

Jolly, W.M., Nemani, R., Running, S.W., 2005. A generalized, bioclimatic index to predict foliar phenology in response to climate. Global Change Biology 11, 619–632.

Liang, L., Schwartz, M.D., Fei, S., 2011. Photographic assessment of temperate forest understory phenology in relation to springtime meteorological drivers. International Journal of Biometeorology 56, 343–355.

Litwin, D., Tjahjadi, T., Yang, Y.-H., 2001. Colour image segmentation using optical models. In: Pluta, M. (Ed.), Proceedings of SPIE in Optical Sensing for Public Safety, Health, and Security, 4535, pp. 137–144.

Morisette, J.T., Richardson, A.D., Knapp, A.K., Fisher, J.I., Graham, E.A., Abatzoglou, J., Wilson, B.E., Breshears, D.D., Henebry, G.M., Hanes, J.M., Liang, L., 2009. Tracking the rhythm of the seasons in the face of global change: phenological research in the 21st century. Frontiers in Ecology and the Environment 7, 253–260.

Panneton, B., Brouillard, M., 2009. Colour representation methods for segmentation of vegetation in photographs. Biosystems Engineering 102, 365–378.

R Development Core Team, 2012. R: a language and environment for statistical computing. R Foundation for Statistical Computing, Vienna, Austria3-900051-07-0 (URL: http://www.R-project.org).

Richardson, A.D., Jenkins, J.P., Braswell, B.H., Hollinger, D.Y., Ollinger, S.V., Smith, M.-L., 2007. Use of digital webcam images to track spring green-up in a deciduous broadleaf forest. Oecologia 152, 323–334.

Root, T.L., Price, J.T., Hall, K.R., Schneider, S.H., Rosenzweig, C., Pounds, J.A., 2003. Fingerprints of global warming on wild animals and plants. Nature 421, 57–60.

Schwartz, M.D., Betancourt, J.L., Weltzin, J.F., 2012. From Caprio's lilacs to the USA National Phenology Network. Frontiers in Ecology and the Environment 10, 324–327.

Slaughter, D.C., Giles, D.K., Downey, D., 2008. Autonomous robotic weed control systems: a review. Computers and Electronics in Agriculture 61, 63–78.

Slayback, D.A., Pinzon, J.E., Los, S.O., Tucker, C.J., 2003. Northern hemisphere photosynthetic trends 1982–99. Global Change Biology 9, 1–15.

Song, D., Qin, N.I., Goldberg, K., 2006. A minimum variance calibration algorithm for pan–tilt robotic cameras in natural environments. Proceedings 2006 IEEE International Conference on Robotics and Automation, 2006, pp. 3449–3456 (ICRA 2006).

Sonnentag, O., Hufkens, K., Teshera-Sterne, C., Young, A.M., Friedl, M., Braswell, B.H., Milliman, T., O'Keefe, J., Richardson, A.D., 2011. Digital repeat photography for phenological research in forest ecosystems. Agricultural and Forest Meteorology 152, 159–177.

Stöckli, R., Vidale, P.L., 2004. European plant phenology, climate as seen in a 20 year AVHRR land-surface parameter dataset. International Journal of Remote Sensing 25, 3303–3330.

Swain, K.C., Nørremark, M., Jørgensen, R.N., Midtiby, H.S., Green, O., 2011. Weed identification using an automated active shape matching (AASM) technique. Biosystems Engineering 110, 450–457.

Walther, G.R., Post, E., Convey, P., Menzel, A., Parmesan, C., Beebee, T.J.C., Fromentin, J.M., Hoegh-Guldberg, O., Bairlein, F., 2002. Ecological responses to recent climate change. Nature 416, 389–395.

Wiwart, M., Fordonski, G., Zuk-Golaszewska, K., Suchowilsda, E., 2008. Early diagnostics of macronutrient deficiencies in three legume species by color image analysis. Computers and Electronics in Agriculture 65, 125–132.

Woebbecke, D.M., Meyer, G.E., Von Bargen, K., Mortensen, D.A., 1995. Color indices for weed identification under various soil, residue, and lighting conditions. Transactions of ASAE 38, 259–269.

Wright, S.J., Carrasco, C., Calderón, C., Paton, S., 1999. The El Niño southern oscillation, variable fruit production, and famine in a tropical forest. Ecology 80, 1632–1647.